ISSN: 0000-0000 www.aristonpubs.com/sciengg-advances https://doi.org/10.69626/sea.2024.0048

RESEARCH ARTICLE

Eco-Friendly Synthesis and Properties of Zinc Oxide Nanoparticles Using *Ocimum tenuiflorum* Leaf Extract

Ravi Kumar [1], Naveen Thakur [2,3], Saurabh Sharma [4], Kuldeep Kumar [1,3,*]

ABSTRACT: This study explores the green synthesis of zinc oxide nanoparticles (ZnO NPs) using the leaf extract of *Ocimum tenuiflorum* as a reducing agent. Characterization of the synthesized ZnO NPs was performed using UV-visible spectroscopy, Scanning electron microscopy (SEM), Transmission electron microscopy (TEM), and X-ray diffraction (XRD). The UV-visible absorption spectrum revealed maximum absorption peaks at 342 and 365 nm for ZnO NPs synthesized with 0.5 and 1.5 mmol.kg^{-1} zinc nitrate concentrations, yielding bandgap energies (E_g) of 3.62 and 3.39 eV, respectively. XRD analysis confirmed the crystalline nature of the ZnO NPs, exhibiting dominant peaks corresponding to the hexagonal wurtzite structure. The average crystalline sizes, were found to be 15.04 and 22.16 nm for the 0.5 and 1.5 mmol·kg^{-1} concentrations of zinc nitrate, respectively. The SEM/TEM micrographs revealed that the nanoparticles have a roughly spherical-like morphology with an average size of 40-50 nm. The synthesized materials were examined for their photocatalytic activity towards the degradation of methyl orange (MO) dye. These findings demonstrate an eco-friendly method for synthesizing ZnO NPs with controlled properties suitable for various applications. Thus, the ZnO nanoparticles synthesized by using such type of eco-friendly method can be used for carrying out pharmaceutical research and therapeutic application in the future.

Keywords: Green synthesis, Zinc oxide nanoparticles, *Ocimum tenuiflorum*, UV-visible spectroscopy, X-ray diffraction

Received: 13 February 2024; Revised: 27 March 2024; Accepted: 03 May 2024; Available Online: 21 May 2024

1. INTRODUCTION

In the realm of nanotechnology, nanoparticles play a pivotal role in numerous applications due to their superior properties compared to bulk materials, including enhanced conductivity, magnetic properties, mechanical strength, and thermal stability [1]. Nanoparticles are utilized in a wide array of fields. Nanotechnology involves the manipulation and production of chemical, physical, and biological systems at scales ranging from individual molecules or atoms to submicron dimensions, as well as the integration of the resulting nanostructures into larger systems [2]. This technology is poised to have a profound impact on our economy and society in the early 21st century, comparable to the transformative effects of semiconductor technology, information technology, cellular and molecular biology, and medical sciences [3]. Research in nanotechnology promises breakthroughs in areas such as material manufacturing, nanoelectronics, energy, pharmaceuticals, biotechnology, and information technology. It is widely anticipated that nanotechnology will drive the next Industrial Revolution [4, 5]. Nanomaterials are typically classified into four groups: zero, one, two, and three-dimensional structures [1]. Zero-dimensional nanostructures, often referred to as quantum

[1] Department of Chemistry, Career Point University, Hamirpur-176041, Himachal Preadesh, India
[2] Department of Physics, Career Point University, Hamirpur-176041, Himachal Pradesh, India
[3] Centre for Nano-Science and Technology, Career Point University, Hamirpur-176041, Himachal Pradesh, India
[4] Thakur PG College of Education, Dhaliara, Kangra-177103, Himachal Pradesh, India

* Author to whom correspondence should be addressed: kuldeep.sharma.753@gmail.com (Kuldeep Kumar)

dots or nanoparticles with an aspect ratio near unity, have been extensively utilized in biological applications. One-dimensional structures include a diverse range of forms such as needles, helices, nanorods, ribbons, belts, wires, and combs. Zinc oxide (ZnO) can form two-dimensional structures such as nanopellets and nanosheets or nanoplates [5, 6]. Examples of three-dimensional ZnO structures include snowflakes, dandelions, and flowers.

Despite the potential applications of NPs in the development of novel technologies, their synthesis is an expensive process and requires specific separation techniques from aqueous solutions. Due to increased demand for various metallic and non-metallic NPs over the past two decades, a wide range of physical and chemical techniques have been developed to produce nanoparticles of different sizes, shapes and compositions [7, 8]. Various physical, biological and chemical synthesis methods have been followed for obtaining these metal oxide nanoparticles and among them chemical synthetic route is widely accepted which uses a range of inorganic and organic reducing agents [9]. Chemical synthesis methods include emulsion solvent extraction method, double emulsion and evaporation method, salting out method, emulsion diffusion method and solvent displacement/precipitation method [10].

Zinc oxide have many and very impressive properties like wide band gap, high piezoelectric property, large binding energy etc. It is used in large number of applications like, optoelectronic devices, electromagnetic coupled sensor, laser devices, surface acoustic wave device [4-8]. Zinc oxide nanoparticles have been used to eliminate sulphur, arsenic from water because bulk ZnO cannot remove arsenic because nanoparticles have great surface area than bulk material. Zinc oxides have amazing application in diagnostics, bimolecular detection, micro-electronic [10]. Zinc oxide can occur in two-dimensional structures such as nano pellets, nanosheet/nanoplates. Examples of three-dimensional structures of ZnO include snowflakes, dandelion and flower. Among the metal oxide nanoparticles, zinc oxide is interesting because it has vast applications in various areas such as optical, piezoelectric, magnetic, and gas sensing. Beside these properties, ZnO nanostructure exhibits high catalytic efficiency, strong adsorption and are used frequently in the manufacture of sunscreens [11] ceramics, and rubber processing, waste water treatment, and as a fungicide [12, 13]. In fact, the ZnO usage may overtake nano-titanium dioxide (TiO_2) as it can absorb both UV-A and UV-B radiation while TiO_2 can only block UV-B, and therefore offering better protection and improved opaqueness. ZnO has large excitation binding energy (60 meV) which allows UV lasing action to occur even at room temperature [14] and ZnO with Oxygen vacancies exhibits an efficient green emission.

In this study, we present the synthesis of ZnO nanoparticles using varying concentrations of precursor salts in *Ocimum tenuiflorum* leaf extract. The photocatalytic activity of the synthesized ZnO nanoparticles was evaluated for the degradation of methylene orange (MO) dye.

2. EXPERIMENTAL DETAILS

2.1 Materials

The highly pure chemicals sodium hydroxide and zinc nitrate have been purchased from Fizmerk India Chemicals and Nice. Chemicals Ltd., respectively. These chemicals have been used as received without further purification. Distilled water with conductivity 0.05 Scm^{-1} and pH=7 has been used for all experiments. The *Ocimum tenuiflorum* leaves will collect from nearby area of the Career Point University, Hamirpur.

2.2. Preparation of leaf extract of *Ocimum tenuiflorum*

In preparation of leaf extract of *Ocimum tenuiflorum*, firstly leaves washed with distilled water. Then the dried 10g leaves have been placed in 250 ml borosil for 20 minutes until solution color turns reddish. The mixture solution cooled at room temperature. After cooling, the leaf extract filtered. The filtered extract then stored in refrigerator for synthesis of ZnO NPs.

2.3. Synthesis of ZnO NPs by using *Ocimum tenuiflorum* leaf extract

For the synthesis of ZnO NPs, 30 ml of *Ocimum tenuiflorum* leaf extract will heat up to maintain temperature in the range 60-80° C using magnetic stirrer heater. Then 0.5, 1.5 and Zinc nitrate solution has been added to above leaf extract of *Ocimum tenuiflorum* and the mixture is then at 70° C until it reduced to deep reddish paste. The pH of the mixture is maintained at 11 by using 1 $mol.kg^{-1}$ NaOH solution. After this, the paste dried at temperature 100-130° C for 40-45 minutes. ZnO NPs attained in form of light in the form of light-yellow colored powder and mashed in ceramic mortar pestle to get finer nature for characterization purposes.

3. RESULTS AND DISCUSSION

3.1. UV-visible spectroscopy

The absorption spectrum of the synthesized ZnO nanoparticles (NPs) was examined using UV-visible absorption spectroscopy. The UV-vis spectra, as depicted in Figure 1, reveal characteristic absorption peaks for the synthesized ZnO NPs at 342 nm and 365 nm. These spectra were further utilized to determine the optical energy band gap (Eg) using the well-known relation mentioned below [15]:

$$E_g = \frac{hc}{\lambda}$$

where, h is Plank's constant = 6.626×10^{-34} Js, c is the speed of light = 3×10^{8} m/s and λ corresponds to the wavelength of the peak with maximum intensity. This relationship is fundamental in solid-state physics and materials science for understanding the electronic properties of semiconductors.

The observed absorption peaks at 342 nm and 365 nm indicate successful synthesis of ZnO NPs with distinct optical properties. The optical energy band gap (Eg) values calculated from these peaks are presented in Table 1. It is

evident from the data that the Eg values decrease with increasing concentration of $Zn(NO_3)_2$. Specifically, the band gap decreases from 3.62 eV to 3.39 eV as the concentration of $Zn(NO_3)_2$ increases from 0.5 mmol·kg^{-1} to 1.5 mmol·kg^{-1}.

This decrease in Eg can be attributed to the quantum confinement effect, which is influenced by the size of the nanoparticles. As the size of the ZnO NPs increases, the band gap decreases due to the reduced quantum confinement effect in larger particles. This size-dependent band gap variation is a critical factor in tailoring the electronic and optical properties of ZnO NPs for specific applications, such as in optoelectronic devices, sensors, and photocatalysts.

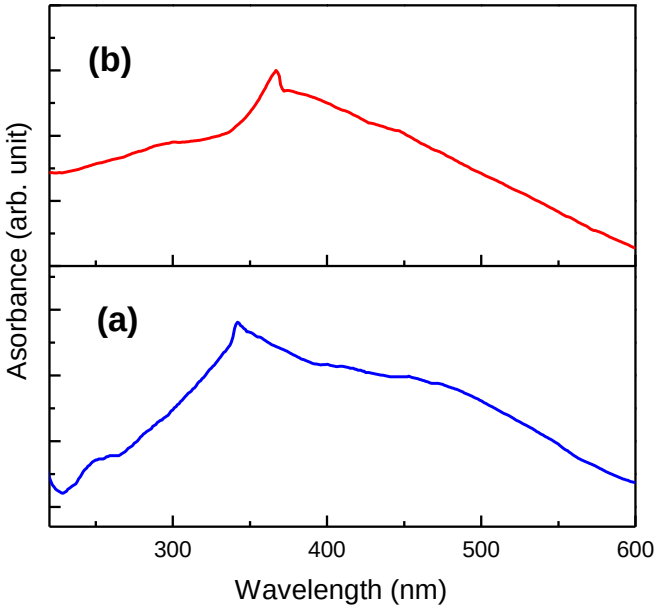

Fig. 1. UV-Visible spectra of ZnO nanoparticles synthesized using (a) 0.5 and (b) 1.5 mmol·kg^{-1} $Zn(NO_3)_2$.

Table 1. λmax and energy band gap (Eg) values of ZnO nanoparticles synthesized using different concentrations of $Zn(NO_3)_2$.

$Zn(NO_3)_2$ (mmol·kg^{-1})	λmax (nm)	Eg (eV)
0.5	342	3.62
1.5	365	3.39

3.2. XRD analysis

The X-ray diffraction (XRD) patterns of the as-prepared ZnO nanoparticle samples are shown in Fig. 2. The XRD peaks for each sample appear at 2θ angles of approximately 31.9°, 34.5°, 36.3°, 47.6°, 56.7°, 62.9°, 66.0°, 68.0°, and 69.2°. These peaks correspond to the (100), (002), (101), (102), (110), (103), (200), (112), and (201) crystal planes, respectively, and can be accurately indexed to a hexagonal wurtzite structure of ZnO, as per the Joint Committee on Powder Diffraction Standards (JCPDS) card # 05-0664 and supported by previous studies [16, 17]. The absence of any extraneous peaks in the XRD spectra confirms the phase purity of all synthesized samples, indicating that the samples are free from impurities and secondary phases. This purity is crucial for applications that rely on the intrinsic properties of ZnO, such as optoelectronic devices and sensors.

Additionally, the intensity of the major diffraction peaks at 2θ angles of 31.9°, 34.5°, and 36.3° remains unaffected by the concentration of the precursor, $Zn(NO_3)_2$, suggesting that the crystallinity of the ZnO nanoparticles is consistent across different synthesis conditions [18, 19]. The well-defined, sharp peaks in the XRD patterns indicate that the as-prepared ZnO samples are highly crystalline. The crystallite size (D) was determined using the Scherrer equation [20-22]:

$$D = \frac{K\lambda}{\beta Cos\theta}$$

where K is the shape factor (typically 0.9 for spherical particles), λ is the X-ray wavelength (1.5406 Å for Cu-Kα radiation), β is the full width at half maximum (FWHM) of the peak, and θ is the Bragg angle. The lattice parameters of the hexagonal unit cell were calculated using standard crystallographic relations and the inter-planar spacing (d) was determined from Bragg's law [21, 22]:

$$2dsin\theta = n\lambda$$

The results, summarized in Table 2, show that the crystallite size increases with the concentration of $Zn(NO_3)_2$, from 15.04 nm at 0.5 mmol·kg^{-1} to 22.16 nm at 1.5 mmol·kg^{-1}. However, there is no significant variation in the inter-planar spacing d, lattice parameters or unit cell volume V with changes in the precursor concentration, indicating that the basic crystal structure of ZnO remains unaffected by the synthesis conditions.

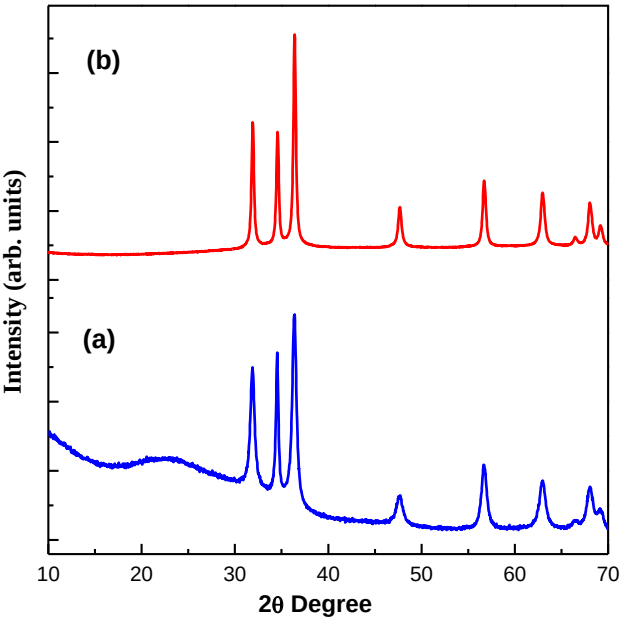

Fig. 2. XRD spectra of ZnO nanoparticles synthesized using (a) 0.5 and (b) 1.5 mmol·kg^{-1} $Zn(NO_3)_2$.

Table 2. Crystallite size (D), inter-planar spacing (d), lattice parameters (a = b and c), and volume (V) calculated from XRD measurements at different concentrations of $Zn(NO_3)_2$.

$Zn(NO_3)_2$ (mmol·kg^{-1})	D (nm)	d (nm)	a = b (nm)	c (nm)	V (nm^3)
0.5	15.04	0.2467	0.3238	0.5189	4.710
1.5	22.16	0.2465	0.3234	0.5183	4.695

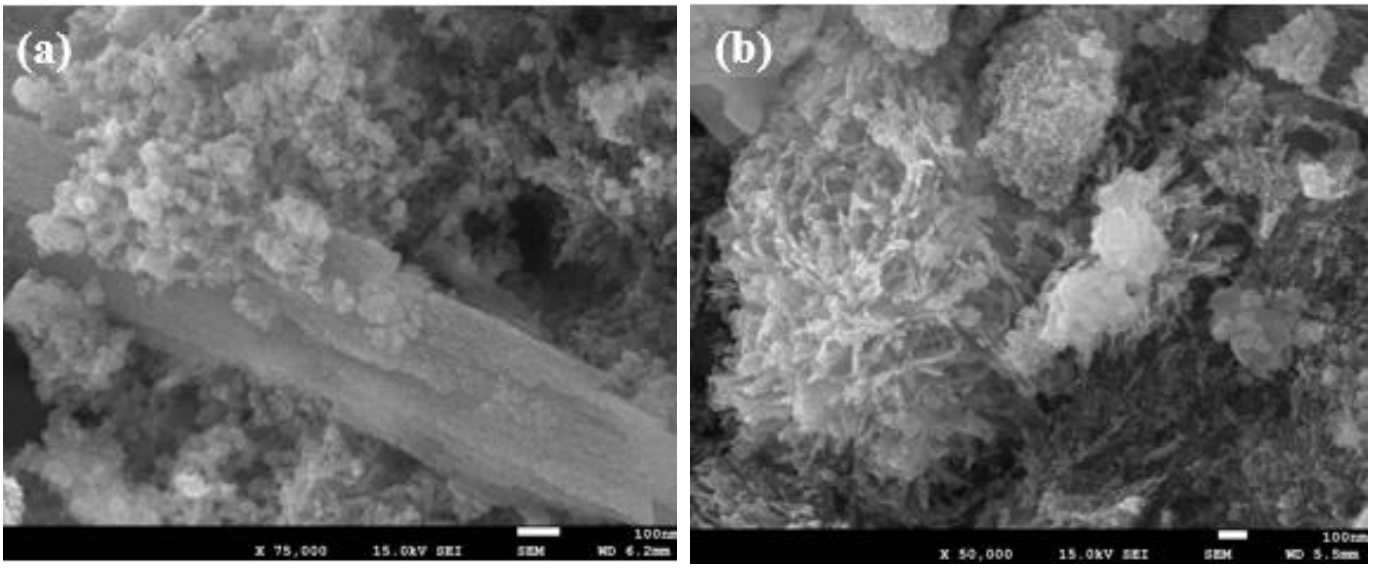

Fig. 3. SEM images of ZnO nanoparticles synthesized using (a) 0.5 and (b) 1.5 mmol·kg^{-1} $Zn(NO_3)_2$.

3.3. Scanning Electron Microscopy

Scanning electron microscopy (SEM) provides detailed insights into the shape and surface morphology of synthesized ZnO nanoparticles (NPs). This technique is particularly effective for analyzing surface features and size distribution, offering high-resolution images that reveal the nanostructures' intricate details. The SEM images of ZnO nanoparticles synthesized with different concentrations of $Zn(NO_3)_2$ are shown in Figure 3 (a) and (b). These images reveal that the nanoparticles exhibit a roughly small spherical and coral reef-like morphology. The spherical shape and coral reef-like structures suggest a high surface area, which is beneficial for applications such as catalysis and sensing. The SEM images in Figure 3 (a) for ZnO nanomaterial synthesized using 0.5 mmol·kg^{-1} $Zn(NO_3)_2$ show predominantly small spherical nanoparticles with some agglomeration, characteristic of a high surface energy and potential for various applications. In contrast, Figure 3 (b) for ZnO NPs synthesized using 1.5 mmol·kg^{-1} Zn(NO3)2 reveals a more defined coral reef-like morphology, which can provide a larger active surface area, enhancing the material's reactivity and interaction with other substances. The ability to control and manipulate the morphology of ZnO nanoparticles through different synthesis methods and precursor concentrations is crucial for optimizing their performance in specific applications. This morphological versatility makes ZnO nanoparticles suitable for a wide range of applications, including photocatalysis, biomedical applications, and electronic devices.

3.4 Transmission Electron Microscopy

The microstructural features of the synthesized ZnO nanoparticles were further investigated using transmission electron microscopy (TEM), with the results presented in Figure 4. TEM provides high-resolution images that offer detailed insights into the internal structure and morphology of nanoparticles, complementing the observations made with SEM. The TEM images reveal that the ZnO nanoparticles synthesized at different precursor concentrations exhibit a small spherical morphology, similar to the shapes observed in the SEM images. This consistency between SEM and TEM results confirms the robustness of the synthesis method in producing nanoparticles with uniform shapes and sizes. Notably, the TEM images highlight the influence of precursor concentration on the structure and morphology of ZnO nanoparticles. At both precursor concentrations of 0.5 mmol·kg^{-1} and 1.5 mmol·kg^{-1} $Zn(NO_3)_2$, the nanoparticles maintain a small spherical shape, indicating that the precursor concentration is crucial in tuning the morphology without significantly altering the crystallite structure. The average size of these nanoparticles is found to be approximately 10-40 nm, which is consistent across different precursor concentrations.

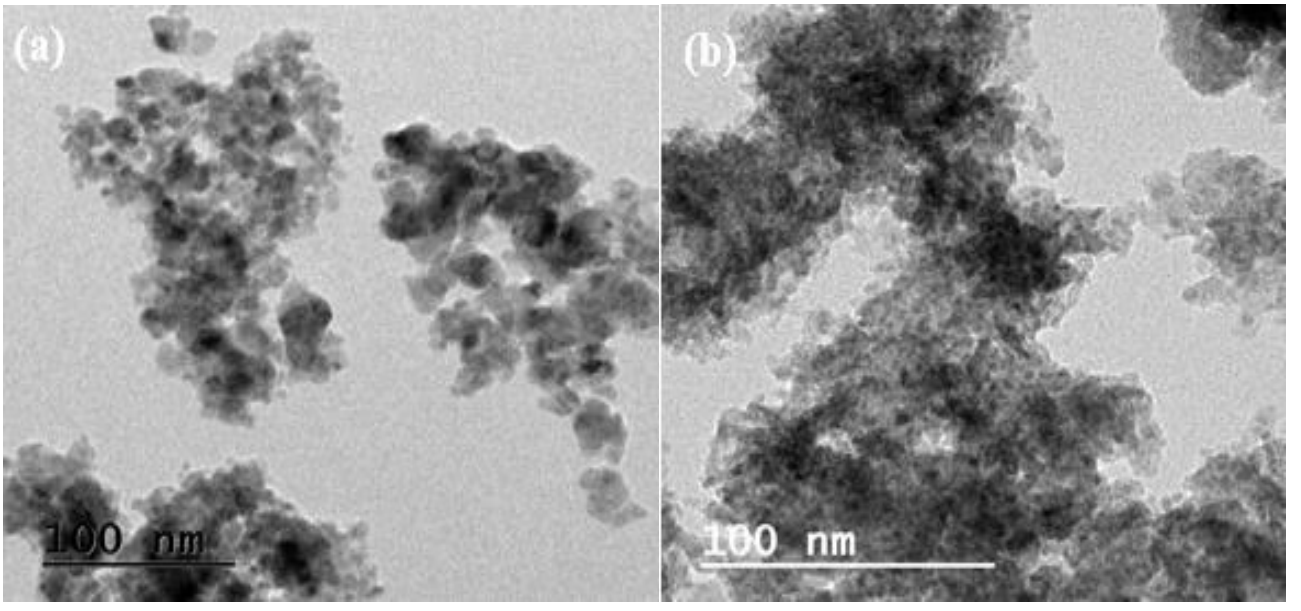

Fig. 4. TEM images of ZnO nanoparticles synthesized using (a) 0.5 and (b) 1.5 mmol·kg^{-1} $Zn(NO_3)_2$.

Similar findings have been reported in the literature. For instance, Wang et al. observed distorted spherical-shaped ZnO nanoparticles and explained that the shape of ZnO NPs changed from rods to globular as the concentration of $ZnCl_2$ solution increased [23]. This study further supports the observation that precursor concentration can significantly influence the morphology of ZnO nanoparticles while maintaining their crystalline structure. The ability to control the size and shape of ZnO nanoparticles through variations in precursor concentration is essential for optimizing their properties for specific applications. The small spherical morphology observed in the TEM images suggests a high surface area, which is advantageous for applications such as catalysis, drug delivery, and sensing technologies.

3.5. Photocatalytic Activity

The photocatalytic activity of the synthesized ZnO nanoparticles (NPs) was evaluated by examining the degradation of a 10 ppm aqueous solution of Methyl Orange (MO) dye. MO dye, known for its highly intense peak at 465 nm in the UV-visible spectrum, served as a model contaminant. The degradation process was carried out under UV-visible light for 180 minutes, and the progress was monitored by measuring the intensity of the peak at 465 nm over time. This method provided a clear indication of the dye degradation, as the intensity of the peak decreased, correlating with the decolorization of the dye solution in the presence of the photocatalyst (Figure 5).

The percentage degradation of the dye was calculated using the following relation:

$$\%\ Degradation = \frac{A_o - A_t}{A_o} \times 100$$

where A_0 is the absorbance of the pure dye solution and A_t is the absorbance of the reaction mixture at time t. The data, presented in Table 3 and illustrated in Figure 6, demonstrate the catalytic efficiency of ZnO NPs at different precursor concentrations and dosages. It is evident that the catalytic efficiency of ZnO NPs synthesized with 0.5 mmol·kg^{-1} $Zn(NO_3)_2$ follows the order of 50 > 100 > 25 mg, whereas for ZnO NPs synthesized with 1.5 mmol·kg^{-1} $Zn(NO_3)_2$, the order of photocatalytic efficiency is 50 ≈ 25 > 100 mg.

The mechanism of photocatalytic action of ZnO NPs is based on the generation of electron-hole pairs on the nanoparticle surface. When ZnO NPs absorb photons with energy equal to or greater than their band gap energy, electrons are excited from the valence band to the conduction band, creating electron-hole pairs. These pairs generate strong oxidizing and reducing agents, such as superoxide anions (O_2^-) and hydroxyl radicals (OH). These reactive species are instrumental in breaking down MO dye molecules into harmless byproducts such as carbon dioxide (CO_2) and water (H_2O).

The efficiency of photocatalysis is significantly influenced by factors such as the catalyst dosage, initial dye concentration, light intensity, and reaction time. The data indicate that an optimal catalyst dosage enhances the degradation rate, while excessive amounts can lead to agglomeration, reducing the effective surface area available for the photocatalytic reaction. The synthesized ZnO NPs exhibit excellent photocatalytic performance, with a notable degradation efficiency, especially at a dosage of 50 mg, demonstrating their potential for practical applications in wastewater treatment and environmental remediation. These results underscore the importance of optimizing synthesis parameters to tailor the properties of ZnO nanoparticles for specific photocatalytic applications.

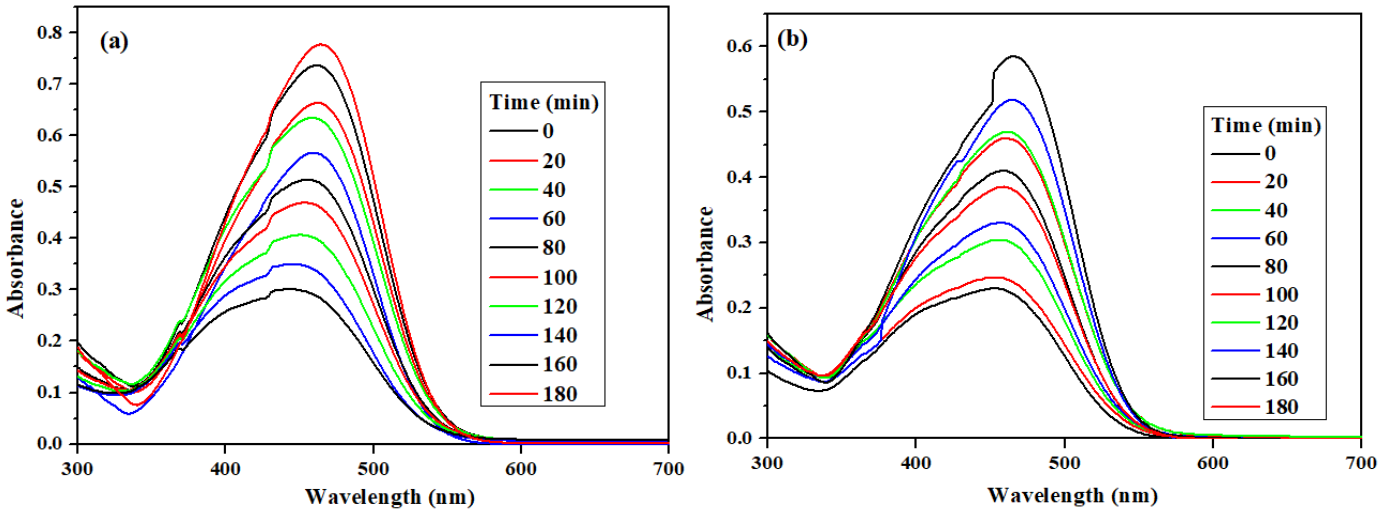

Fig. 5. Typical UV-visible spectra of MO solution (10 ppm) at different time intervals containing 50 mg catalytic load of ZnO NPs synthesized using (a) 0.5 and (b) 1.5 mmol·kg^{-1} $Zn(NO_3)_2$.

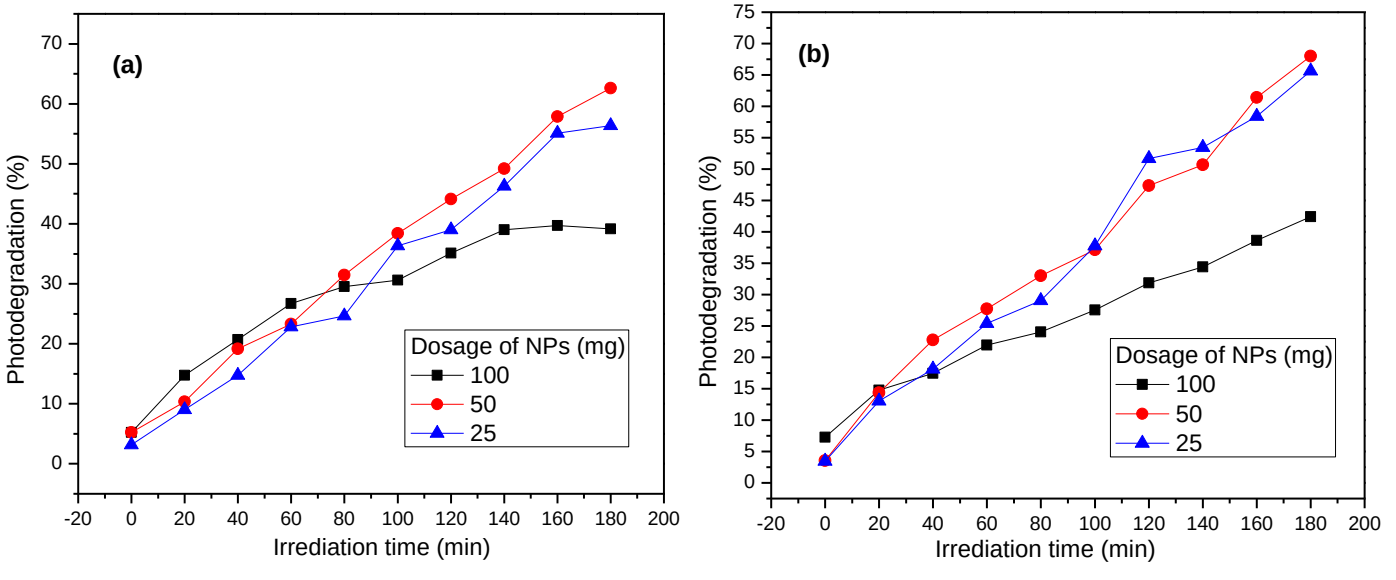

Fig. 6. Percentage photo-degradation of 10 ppm MO dye with time in the presence of ZnO NPs synthesized using (a) 0.5 and (b) 1.5 mmol·kg^{-1} $Zn(NO_3)_2$.

Table 3. Percentage of photocatalytic degradation of 100 ml of 10 ppm MO dye solution at different dosages of ZnO NPs synthesized at different concentrations of $Zn(NO_3)_2$.

[a]m (mmol·kg^{-1})	NPs dosage (mg)	Photocatalytic degradation of MO (%)
0.5	25	56.5
	50	62.4
	100	39.2
1.5	25	65.8
	50	67.9
	100	42.3

[a]m is the molality of zinc nitrate in water

The high surface area and reactivity of ZnO NPs make them suitable candidates for the degradation of organic pollutants, contributing to the development of advanced materials for sustainable environmental technologies.

4. CONCLUSIONS

This study successfully demonstrates the green synthesis of Zinc Oxide nanoparticles (ZnO NPs) using the leaf extract of *Ocimum tenuiflorum* as a reducing agent. The synthesized ZnO NPs were characterized using UV-visible spectroscopy and X-ray diffraction (XRD). UV-visible spectroscopy revealed distinct absorption peaks and bandgap energies for ZnO NPs synthesized with different concentrations of zinc nitrate, indicating effective synthesis and size control. XRD analysis confirmed the crystalline nature of the nanoparticles, showing the hexagonal wurtzite structure and varying crystalline sizes dependent on the concentration of zinc nitrate used. Scanning Electron Microscopy (SEM) and Transmission Electron Microscopy (TEM) micrographs revealed that the nanoparticles have a roughly small spherical-like morphology with an average size of 40-50 nm. The synthesized materials were examined for their photocatalytic activity towards the degradation of methyl orange (MO) dye. The photocatalytic tests showed that ZnO NPs could effectively degrade MO dye, highlighting their potential for environmental remediation. The green synthesis method employed is eco-friendly and cost-effective, utilizing readily available natural resources and simple procedures. This method provides a sustainable approach for the synthesis of ZnO NPs with potential applications in various fields, including electronics, photonics, and biomedical engineering. The study highlights the efficacy of using *Ocimum tenuiflorum* leaf extract in producing ZnO NPs with desirable optical and structural properties, paving the way for further research and development in green nanotechnology. The successful green synthesis of Zinc Oxide nanoparticles using *Ocimum tenuiflorum* leaf extract points to several promising future research directions. Optimizing synthesis parameters and employing advanced characterization techniques could enhance control over nanoparticle properties. Investigating toxicity, biocompatibility, and environmental impact will be crucial for biomedical and environmental applications. Scaling up production methods and evaluating commercial viability will facilitate broader use. Comparative studies with other synthesis methods and integrating ZnO NPs with other materials could lead to innovative applications in drug delivery, biosensors, photocatalysis, and nanocomposites. These efforts will advance sustainable and green nanotechnology, contributing to the development of eco-friendly and efficient technologies for various applications.

CONFLICT OF INTEREST

The authors declare that there is no conflict of interests.

REFERENCES

[1] Bhushan, B., **2017**. Introduction to nanotechnology. *Springer handbook of nanotechnology*, pp.1-19. Springer, Berlin, Heidelberg

[2] Stark, W.J., Stoessel, P.R., Wohlleben, W. and Hafner, A.J.C.S.R., **2015**. Industrial applications of nanoparticles. *Chemical Society Reviews*, *44*(16), pp.5793-5805.

[3] De, M., Ghosh, P.S. and Rotello, V.M., **2008**. Applications of nanoparticles in biology. *Advanced Materials*, *20*(22), pp.4225-4241.

[4] Salata, O.V., **2004**. Applications of nanoparticles in biology and medicine. *Journal of Nanobiotechnology*, 2, pp.1-6.

[5] Parihar, V., Raja, M. and Paulose, R., **2018**. A brief review of structural, electrical and electrochemical properties of zinc oxide nanoparticles. *Reviews on Advanced Materials Science*, *53*(2), pp.119-130.

[6] Saleem, S., Jameel, M.H., Rehman, A., Tahir, M.B., Irshad, M.I., Jiang, Z.Y., Malik, R.Q., Hussain, A.A., ur Rehman, A., Jabbar, A.H. and Alzahrani, A.Y., **2022**. Evaluation of structural, morphological, optical, and electrical properties of zinc oxide semiconductor nanoparticles with microwave plasma treatment for electronic device applications. *Journal of Materials Research and Technology*, *19*, pp.2126-2134.

[7] Zhang, Y., Yang, Y., Zhao, J., Tan, R., Wang, W., Cui, P. and Song, W., **2011**. Optical and electrical properties of aluminum-doped zinc oxide nanoparticles. *Journal of Materials Science*, *46*, pp.774-780.

[8] Kulkarni, S.S. and Shirsat, M.D., **2015**. Optical and structural properties of zinc oxide nanoparticles. *International Journal of Advanced Research in Physical Science*, *2*(1), pp.14-18.

[9] Choi, A., Kim, K., Jung, H.I. and Lee, S.Y., **2010**. ZnO nanowire biosensors for detection of biomolecular interactions in enhancement mode. *Sensors and Actuators B: Chemical*, *148*(2), pp.577-582.

[10] Raha, S. and Ahmaruzzaman, M., **2022**. ZnO nanostructured materials and their potential applications: progress, challenges and perspectives. *Nanoscale Advances*, *4*(8), pp.1868-1925.

[11] Porrawatkul, P., Nuengmatcha, P., Kuyyogsuy, A., Pimsen, R. and Rattanaburi, P., **2023**. Effect of Na and Al doping on ZnO nanoparticles for potential application in sunscreens. *Journal of Photochemistry and Photobiology B: Biology*, *240*, p.112668.

[12] Jiang, J., Pi, J. and Cai, J., **2018.** The advancing of zinc

oxide nanoparticles for biomedical applications. *Bioinorganic Chemistry and Applications*, *2018*(1), p.1062562.

[13] Talam, S., Karumuri, S.R. and Gunnam, N., **2012.** Synthesis, characterization, and spectroscopic properties of ZnO nanoparticles. *International Scholarly Research Notices*, *2012*(1), p.372505.

[14] Mishra, S.K., Srivastava, R.K. and Prakash, S.G., **2012.** ZnO nanoparticles: Structural, optical and photoconductivity characteristics. *Journal of Alloys and Compounds*, *539*, pp.1-6.

[15] Srivastava, V., Gusain, D. and Sharma, Y.C., **2013.** Synthesis, characterization and application of zinc oxide nanoparticles (n-ZnO). *Ceramics International*, *39*(8), pp.9803-9808.

[16] Rana, S.B., Singh, P., Sharma, A.K., Carbonari, A.W. and Dogra, R., **2010.** Synthesis and characterization of pure and doped ZnO nanoparticles. *Journal of Optoelectronics and Advanced Materials*, 12(2), p.257.

[17] Joseph, H.M. and Poornima, N., **2019.** Synthesis and characterization of ZnO nanoparticles. *Materials Today: Proceedings*, 9, pp.7-12.

[18] Hameed, A.S.H., Karthikeyan, C., Ahamed, A.P., Thajuddin, N., Alharbi, N.S., Alharbi, S.A. and Ravi, G., **2016.** In vitro antibacterial activity of ZnO and Nd doped ZnO nanoparticles against ESBL producing Escherichia coli and Klebsiella pneumoniae. *Scientific reports*, *6*(1), p.24312.

[19] Khorsand Zak, A., Abd. Majid, W.H., Abrishami, M.E., Yousefi, R. **2011.** X-ray analysis of ZnO nanoparticles by Williamson-Hall and size-strain plot methods. *Solid State Science*. 13:251-256.

[20] Lakshmeesha, T.R., Sateesh, M.K., Prasad, B.D., Sharma, S.C., Kavyashree, D., Chandrasekhar, M. and Nagabhushana, H., **2014.** Reactivity of crystalline ZnO superstructures against fungi and bacterial pathogens: Synthesized using Nerium oleander leaf extract. *Crystal growth & design*, *14*(8), pp.4068-4079.

[21] Samat, A.N., Nor, M.R. **2013.** Sol-gel synthesis of zinc oxide nanoparticles using *Citrus aurantifolia* extracts. *Ceramics International*, 39, pp. 545–548.

[22] Elangovan, S.V., Chandramohan, V., Sivakumar, N., Senthil, T.S. **2016.** Synthesis and characterization of ZnO nanoparticles at different molarity concentrations for photocatalytic applications. *Desalination and Water Treatment*, 57, pp. 9671–9678.

[23] Wang, Z.L. **2004.** Nanostructures of zinc oxide. *Materials Today*, 7(6), pp. 26-33.

